# Determination of Equilibrium Isotherms Using Dynamic Column Breakthrough and Constant Flow Equilibrium Desorption

**A. Malek and S. Farooq***

Department of Chemical Engineering, National University of Singapore, 10 Kent Ridge Crescent, Singapore 119260, Singapore

Reliable adsorption equilibrium data are key elements in the design of an adsorption separation process. Two excellent methods for obtaining single-component equilibrium isotherm data are the dynamic column breakthrough method and the constant flow equilibrium desorption method. Both these methods were used to derive the equilibrium isotherms of methane, ethane, and propane in activated carbon and silica gel. The experimental setup and analysis required for these methods are elaborated. The equilibrium results for these gases for a moderate pressure range and at three different temperatures are presented.

## Introduction

Obtaining reliable adsorption equilibrium data is crucial since the isotherms so derived generally form the basis for further adsorption process design and engineering. This is particularly apparent in the design of pressure-swing adsorption processes. There are a number of methods available to determine adsorption equilibrium data. This paper describes the use of two methods that can be employed to generate single-component equilibrium isotherms over a wide pressure range. One of the more reliable experimental methods for determining equilibrium and kinetic properties of adsorption is the dynamic column breakthrough (DCBT) method. Here, a series of breakthrough curves are generated from a column packed with the adsorbent by giving a step increase in the feed composition to the column. The advantages in using this method are that the analysis is relatively simple and that more representative equilibrium data can be obtained, since it uses a relatively large amount of adsorbent. Of additional importance is that a substantial amount of information on adsorption heat transfer dynamics is also obtainable using this method, especially for systems with high solid loadings and heats of adsorption. However, like many other methods, DCBT is not reliable for deriving equilibrium data at extremely low feed concentrations. This is a shortcoming for systems which exhibit very nonlinear isotherms, since then it is not possible to determine the equilibrium constants in the linear range.

The second method, which can give reliable results in very high pressure ranges, is the constant flow, equilibrium desorption (CFED) method. This method involves the slow desorption of a saturated adsorbent under equilibrium, isothermal conditions. Pure feed is used, and a small but constant flow of the gas is allowed to exit from the system. Thus, the system pressure gradually decreases with time. A material balance performed at suitable intervals of the desorption process provides the equilibrium isotherm profile. Discernibly, the CFED method provides a quick way of obtaining equilibrium data over a wide concentration range. However, this method requires an excellent flow control device, and it is not suitable for adsorbate partial pressures of less than atmospheric pressure.

## Dynamic Column Breakthrough Method

The dynamic column method of measuring single-component isotherm data involves monitoring a series of breakthrough curves in a column packed with the adsorbent. One of the simplest methods is to introduce a step change in the feed concentration of the adsorbable species. This step increase in the concentration of the adsorbable species can be achieved by switching the feed flow of the adsorbate on or off through the use of manual or solenoid valves. Various feed concentrations of the adsorbable component in an inert carrier are normally used in order to obtain the isotherm over a large range of concentrations. Moreover, the step change is not restricted to an increase of between zero to some finite value. The step increase in concentration may be between any two values as long as the condition of equilibrium has been attained before and after each run. The method is usually complemented with the desorption process in order to verify the equilibrium results and also to identify the existence of any hysterisis. In the case of desorption, the adsorbate feed flow is either switched off or reduced.

It is advantageous to keep the feed velocity constant during the switching procedure by correspondingly decreasing or increasing the inert flow. If this is not done, the system hydrodynamics will be unduly disturbed, resulting in ineffective back pressure regulation and hence changes in bed pressure. This is particularly significant when the adsorbate fraction in the feed is high.

From the breakthrough curves, the mean residence time of the adsorption process for that particular operating condition can be derived, from which the equilibrium adsorption capacity may be determined. The derivation of the mean residence time and equilibrium loading using the breakthrough curve follows from a transient material balance. The analysis given below is applicable for experiments using either a regenerated bed for adsorption or complete removal of adsorbed species for desorption. The analysis for nonregenerated bed adsorption and for partial desorption of an equilibrated bed is subsequently introduced, and its merits are discussed.

A further point regarding this method is the need for blank runs. Because the mean residence time integrals are calculated immediately upon effecting the step change in feed concentration, the integral value has to be corrected for the piping volume and other dead space in the experimental setup. The best way of doing this is to perform a blank run using the same experimental conditions, but bypassing the adsorbent bed.

***Analysis of Breakthrough Curves.*** For experiments involving only trace components of the adsorbable species,

* To whom correspondence should be addressed.

0021-9568/96/1741-0025$12.00/0 

there is very little change in velocity and pressure in the system. Thus, we can assume that the inlet and exit flow rates, $q_i$ and $q_e$, respectively, are equal and that the bed pressure, $P_B$, is constant. In this case, the mean residence time, $\tau_a$, is given by the following well-known formula:

$$\tau_a = \int_0^{t^\infty} (1 - x_{ae}/x_{ai})\, dt \tag{1}$$

where $x_{ai}$ is the inlet adsorbate mole fraction and $x_{ae}$ is the outlet adsorbate mole fraction.

For adsorption to a regenerated bed, the equilibrium adsorption capacity, $q^*$, corresponding to the partial pressure, $P_B x_{ai}$, of the adsorbate in the feed can be derived from the adsorbate material balance, giving

$$q^* = \left(\frac{(v_i \tau_a)}{L} - 1\right)\frac{\epsilon}{1-\epsilon}\frac{C_{ai}}{\rho_p} \tag{2}$$

where $v_i$ is the interstitial gas velocity, $L$ bed length, $\epsilon$ is the bed voidage, $C_{ai} = P_B x_{ai}/RT$, $T$ is the column temperature, and $\rho_p$ is the particle density.

For nontrace conditions, where the adsorbate fraction is appreciable, the mean residence time expression has to be corrected for transient velocity changes as well as pressure changes, if any. In this case, the transient sorbate material balance for a regenerated bed with the initial amount of adsorbate in the system being zero is

$$\frac{P_i q_i x_{ai}}{RT} - \frac{P_e q_e x_{ae}}{RT} = \frac{\epsilon V}{RT}\left(\frac{x_a\, dP_B}{dt} + \frac{P_B\, dx_a}{dt}\right) + (1-\epsilon)V\rho_p \frac{dq^*}{dt} \tag{3}$$

where $P_i$ and $P_e$ are the inlet and exit gas pressures, respectively, $V$ is the total column volume, and $x_a$ is the adsorbate mole fraction in the bed (gas phase).

In the equation above, $x_a$ is a variable function of time and axial distance. Integrating eq 3 gives

$$\frac{\epsilon V}{RT}P_f x_{ai} + (1-\epsilon)V\rho_p q^* = \frac{P_i q_i x_{ai}}{RT}\int_0^{t^\infty}\left(1 - \frac{x_{ae} q_e P_e}{x_{ai} q_i P_i}\right) dt \tag{4}$$

While $P_f$ is the final equilibrium bed pressure (equal to $P_B$ if the bed pressure does not vary during the run), $P_e$ and $P_i$ are the exit and inlet pressures, respectively, and can generally be assumed equal, since the bed pressure drop in this case is negligible. In eq 4, the term $P_i q_i$ is constant if a pressure-compensating mass flow controller is used in the adsorption experiments. This allows the molar feed flow term, $P_i q_i x_{ai}/RT$, to be taken out of the integral. The integral term is effectively the mean holding time, and since this is a closed system, it is also the mean residence time. Hence, it is apparent that the general equivalent mean residence time definition for adsorption is

$$\tau_a = \int_0^{t^\infty}\left(1 - \frac{x_{ae} q_e P_e}{x_{ai} q_i P_i}\right) dt \tag{5}$$

In eq 5, the exit flow rate must be known throughout the transient response. If high adsorbate concentrations are used, then $q_e$ will vary with the transient response, being equal to $q_i$ only at the final steady state for the adsorption process. If the flow rate is not measured using a flow sensor, then it has to be approximated on the basis of the material balance equations. Furthermore, where high system pressures are used, depending on the effectiveness of the back pressure regulation, it is also likely that the bed pressure will vary with the transient response. The following analysis shows how to perform the mean residence time analysis where secondary dynamics are introduced into the system due to nontrace conditions. The total material balance for the column is

$$\frac{P_i q_i}{RT} - \frac{P_e q_e}{RT} = \frac{\epsilon V}{RT}\frac{dP_B}{dt} + (1-\epsilon)V\rho_p \frac{dq^*}{dt}$$

or

$$q_e P_e = q_i P_i - \epsilon V \frac{dP_B}{dt} - (1-\epsilon)VRT\rho_p \frac{dq^*}{dt} \tag{6}$$

The expression for $q_e$ above is complicated by the presence of the term involving the adsorption capacity, $q^*$, which is exactly the variable being sought experimentally. The term, however, can be obtained from eq 3 as follows:

$$(1-\epsilon)VRT\rho_p \frac{dq^*}{dt} = q_i P_i x_{ai} - q_e P_e x_{ae} - \epsilon V\left(\frac{x_a\, dP_B}{dt} + \frac{P_B\, dx_a}{dt}\right) \tag{3a}$$

Substituting this expression into eq 6 gives

$$q_e P_e = \frac{q_i P_i (1 - x_{ai}) - \epsilon V (1 - x_a)\frac{dP_B}{dt} + \epsilon V \frac{P_B\, dx_a}{dt}}{(1 - x_{ae})} \tag{3b}$$

If this expression is substituted into eq 5, the mean residence time becomes

$$\tau_a = \int_0^{t^\infty}\left(1 - \frac{x_{ae}}{x_{ai} q_i P_i}\,\frac{q_i P_i (1 - x_{ai}) - \epsilon V (1 - x_a)\frac{dP_B}{dt} + \epsilon V \frac{P_B dx_a}{dt}}{(1 - x_{ae})}\right) dt$$
$$= \int_0^{t^\infty}\left(1 - \frac{x_{ae}}{x_{ai}}\frac{(1 - x_{ai})}{(1 - x_{ae})} + \frac{x_{ae}}{x_{ai}}\frac{(1 - x_a)}{(1 - x_{ae})}\frac{\epsilon V}{q_i P_i}\frac{dP_B}{dt} - \frac{x_{ae}}{x_{ai}}\frac{1}{(1 - x_{ae})}\frac{\epsilon V P_B}{q_i P_i}\frac{dx_a}{dt}\right) dt \tag{7}$$

Hence, eq 7 above gives the general definition of mean residence time for nontrace conditions taking into account the secondary dynamics introduced by velocity and pressure changes. In the equation above, $dx_a/dt$ increases monotonically with time upon addition of adsorbate to the bed, and slowly decreases to zero upon complete breakthrough. However, $dP_B/dt$ begins to increase from zero only at the point of breakthrough, eventually returning to zero upon complete breakthrough. Interestingly, during breakthrough the two gradient terms have a propensity of canceling out.

For the case of desorption from a saturated bed, the same mole balance equations are applicable, except that now $q_i C_{ai} = 0$. Hence,

$$\frac{\epsilon V}{RT}P_f x_{ao} + (1-\epsilon)V\rho_p q^* = \frac{P_i q_i x_{ao}}{RT}\int_0^{t^\infty}\frac{x_{ae} q_e P_e}{x_{ao} q_i P_i}\, dt \tag{8}$$

where $x_{ao}$ in the equation denotes the initial equilibrium adsorbate fraction in the column voids. Thus, for desorp-

tion the corrected mean residence time definition is

$$\tau_d = \int_0^{t^\infty} \frac{x_{ae} q_e P_e}{x_{ai} q_i P_i} \, dt \tag{9}$$

As in the adsorption case, we can substitute the expression for $q_e P_e$ based on the mole balance equations as follows:

$$q_e P_e = q_i P_i - \epsilon V \frac{dP_B}{dt} - (q - \epsilon) VRT \frac{dq^*}{dt}$$

$$= \frac{q_i P_i - \epsilon V (1 - x_a) \frac{dP_B}{dt} + \epsilon V \frac{P_B \, dx_a}{dt}}{(1 - x_{ae})} \tag{10}$$

Substituting this last expression into eq 9 gives

$$\tau_d = \int_0^{t^\infty} \left( \frac{x_{ae}}{x_{ai}} \frac{1}{(1 - x_{ae})} - \frac{x_{ae}}{x_{ai}} \frac{(1 - x_a)}{(1 - x_{ae})} \frac{\epsilon V}{q_i P_i} \frac{dP_B}{dt} + \frac{x_{ae}}{x_{ai}} \frac{1}{(1 - x_{ae})} \frac{\epsilon V P_B}{q_i P_i} \frac{dx_a}{dt} \right) dt \tag{11}$$

Where only trace amounts of adsorbate are used, the expression for the desorption mean residence time reduces to the usual form

$$\tau_d = \int_0^{t^\infty} (x_{ae}/x_{ao}) \, dt \tag{12}$$

and

$$(\epsilon V/RT) P_f x_{ao} + (1 - \epsilon) V \rho_p q^* = q_i C_{ao} \tau_d$$

or

$$q^* = \left( \frac{(v_i \tau_d)}{L} - 1 \right) \frac{\epsilon}{1 - \epsilon} \frac{C_{ao}}{\rho_p} \tag{13}$$

In the case of desorption, $q^*$ is the equilibrium solid loading corresponding to the initial sorbate concentration in the gas phase, $C_{ao}$.

For a step increase in concentration in a bed which initially contains an equilibrium solid loading of $q^*_{t_1}$, corresponding to an equilibrium void concentration of $x_{a1}$, eq 3 applies but, on integration, gives

$$\frac{\epsilon V}{RT} (P_{f2} x_{ai2} - P_{f1} x_{a1}) + (1 - \epsilon) V \rho_p (q^*_{t_1} - q^*_{t_2}) = \frac{P_i q_i x_{ai2}}{RT} \int_{t_1}^{t_2} \left( 1 - \frac{x_{ae2} q_e P_e}{x_{ai2} q_i P_i} \right) dt \tag{14}$$

The mean residence time above is the same as defined in eq 7. Thus, eq 14 can be used repeatedly to solve for $q^*_{t_2}$ knowing $q^*_{t_1}$. Similarly for partial desorption, eq 14 above applies, but since $x_{ai2} < x_{a1}$, $q^*_{t_2} < q^*_{t_1}$. The advantage in using this mode of experiment is that less adsorbate is required to obtain the isotherm over a large pressure range for both adsorption and desorption. However, the possible disadvantage of this approach is that any errors incurred in the results of the first few step changes will propagate and magnify through the subsequent experimental results, thereby rendering the entire isotherm erroneous.

***Numerical Solution of the Mean Residence Time for High Feed Concentrations.*** Equations 7 and 11 can only be solved using numerical methods. For adsorption studies, the following variables are known, $q_i$, $P_i$, and $x_{ai}$, while $x_{ae}$ is a measured variable. Depending on the effectiveness of back pressure regulation, the bed pressure can be maintained constant by restricting the fraction of adsorbate to a moderate value (<60% in this case). This eliminates the derivative term involving pressure in the mean residence time expressions. From eq 7, it is apparent that the adsorbate concentration in the bed voids, $x_a$, is also needed. This variable varies with time, being zero at the beginning of adsorption and rising to $x_{ai}$ at equilibrium. One possible approximation for the profile of $x_a$ is to assume that, at the point of breakthrough, the ratio of $x_a$ to the feed concentration, $x_{ai}$, is equal to the fraction of used bed. The value of $x_a$ is then assumed to increase linearly with time up to the point of equilibrium. This gives a constant derivative term $dx_a/dt$ as follows:

$$\frac{dx_a}{dt} = \frac{(\mathrm{FUB}) x_{ai}}{t^\infty - t_b} \tag{15}$$

where FUB = $1 - t_b/\tau_a$ and $t_b$ is the breakthrough time.

On the basis of actual experimental results of hydrocarbon adsorption onto activated carbon, numerical integration of the term involving the derivative of $x_a$ in eq 7 over the entire transient response showed that the contribution of the term toward the total integral is negligible (≪1.0%) for adsorbate fractions of less than 20% while its contribution gradually increased to just below 1.0% for concentrations of up to 60%. Therefore, the term involving $dx_a/dt$ could be ignored without significant loss of accuracy. The effective mean residence time for adsorption can thus be taken as (*1*)

$$\tau_a = \int_0^{t^\infty} \left( 1 - \frac{x_{ae}}{x_{ai}} \frac{(1 - x_{ai})}{(1 - x_{ae})} \right) dt \tag{16}$$

For desorption systems, however, it is not possible to reliably estimate the drop in void concentration, $x_a$, since this variable is now highly dependent on the desorption characteristics. In some cases, the derivative term $dx_a/dt$ can be rather large at the beginning of desorption, thereby contributing to a large correction factor. For this reason, the modification given for the desorption mean residence time is not easily solved. In the experiments conducted here, desorption runs were carried out only for adsorbate concentrations of less than 50%, in which case the mean residence time can be reasonably approximated as (*1*)

$$\tau_d = \int_0^{t^\infty} \frac{x_{ae}}{x_{ai}} \frac{1}{(1 - x_{ae})} \, dt \tag{17}$$

The desorption experiments conducted and analyzed using this mean residence time definition showed excellent agreement with the corresponding adsorption results at the same equilibrium partial pressure (*1*). This suggests that the isotherms are completely reversible.

### Constant Flow, Equilibrium Desorption Method

In the second method employed here, a packed bed of adsorbent is equilibrated with pure adsorbate at a known initial pressure, and then the feed is shut off. The equilibrated bed is then desorbed at a constant, low exit flow rate to maintain equilibrium conditions throughout. The drop in bed pressure with time is then monitored, from which equilibrium data can be derived.

Since there is no feed in this case, the mole balance is given by

$$\frac{q_e P_e}{RT} = \frac{\epsilon V}{RT} \frac{dP_a}{dt} + (1 - \epsilon) V \rho_p \frac{dq^*}{dt} \tag{18}$$

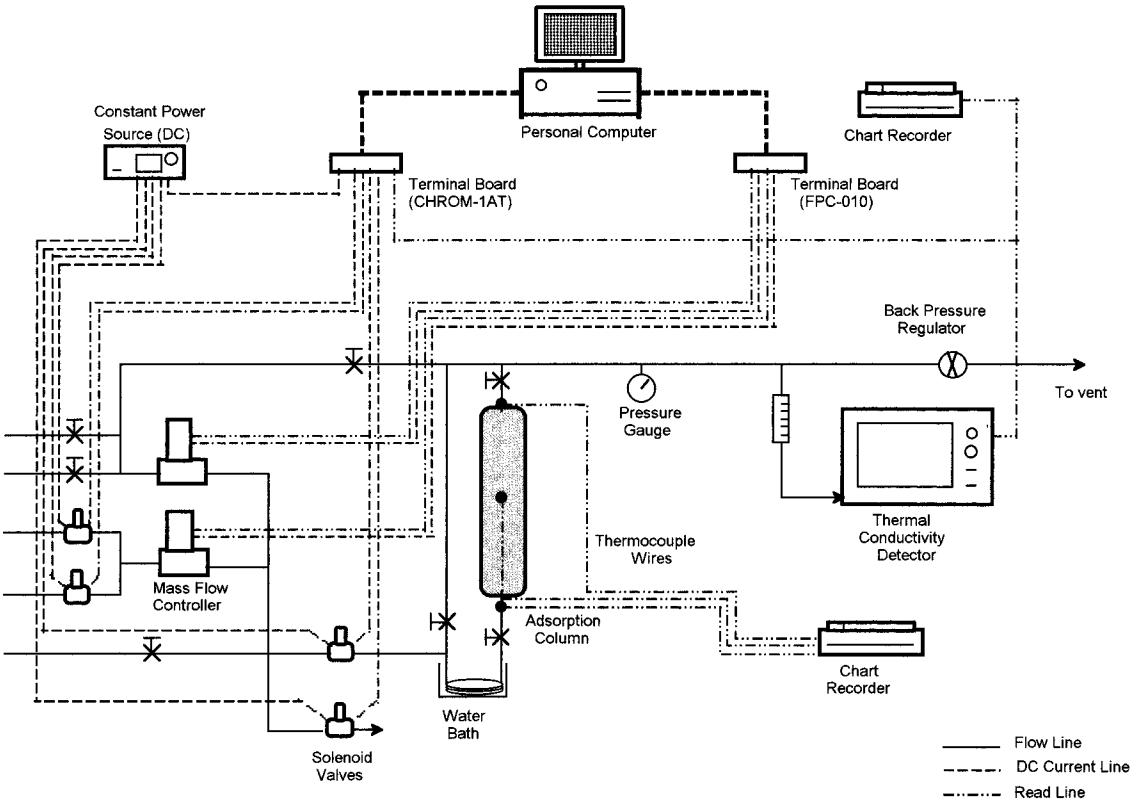


**Figure 1.** Laboratory setup for breakthrough studies.

where $P_a = P_B$ since pure adsorbate is used in the experiments. Integrating eq 18 above gives

$$\frac{\epsilon V}{RT}(P_{Bt_2} - P_{Bt_1}) + (1-\epsilon)V\rho_p(q^*_{t_2} - q^*_{t_1}) = -\frac{q_e P_e}{RT}(t_2 - t_1) \quad (19)$$

The $q_eP_e$ term can be taken out of the integral if a pressure-compensating mass flow controller is used. All the terms in eq 19 are known or measurable except for $q^*_{t_1}$ and $q^*_{t_2}$, the initial and final equilibrium capacities of the bed at high and low pressures, respectively. If one of these is known, then the other can be found from eq 19 above. The normal procedure in using this method is to monitor the pressure profile at regular intervals and to calculate the equilibrium capacity ($q^*_{t_1}$) at a particular pressure backward from a known equilibrium capacity at a low pressure ($q^*_{t_2}$). Equation 19 is thus used repeatedly from the lower bed pressure, $P_{Bt_2}$, to the higher bed pressure, $P_{Bt_1}$. In this regard, the equilibrium capacity at the lowest pressure, $q^*_{t_2}$, must be determined using some other method, for example, the DCBT method. The two methods can thus be complementary, with the DCBT method being used to obtain the equilibrium (as well as kinetic and heat transfer) data for low to moderate pressures and the CFED method being used to extend the isotherm to higher pressures. Discernibly, the CFED method can also be utilized to verify equilibrium results from DCBT experiments.

It should be stressed that equilibrium conditions in the CFED experiments can only be ensured by maintaining a very low exit flow from the bed. Furthermore, results from experiments at different exit flows should be compared in order to confirm that equilibrium conditions are attained.

## Experimental Apparatus

Figure 1 shows a schematic diagram of the apparatus used in the equilibrium studies we conducted. The entire experimental setup was designed to minimize the dead space and piping volume. Elaborate data acquisition and control schemes were also implemented in order to achieve excellent experimental accuracy, reliability, and repeatability.

The apparatus mainly comprises a packed column of adsorbent, a concentration detector, and the necessary process control devices. Jacketed stainless steel columns (i.d. 3.5 cm; length 40.0 cm) were used in the DCBT experiments in order to allow the system to approximate an isothermal process. Water from a temperature-regulated tank was circulated through the jacket using a magnetic, centrifugal pump. The feed stream to the adsorbent column was routed through the temperature-regulated water tank in order to maintain consistent isothermal conditions at the entrance to the column.

Three thermocouples were fitted in the bed to measure the temperature profiles of the entrance, midpoint, and exit of the bed during the experiments. They were K-type thermocouples fitted in 1/8 in. stainless steel tubes packed with hardened magnesium oxide to prevent leakage and also to withstand very high temperatures (~600 K). The thermocouple probes were securely positioned along the center line of the column, in contact with the adsorbents. The thermocouple readings were directly connected to a chart recorder through a Rikadenki K-type temperature module (model RPV-25H), which provides an accuracy of ±0.5 °C.

Three mass flow controllers with different flow ranges were used to control gas flow into the column. Two of these controllers were capable of reliably compensating for pressure changes in the system (Brooks 5850E and 5850TR). The third controller is used for low concentration or trace adsorption studies (Porter VCD1000), in which case fluctuations in the system pressure would be negligible. All three controllers were precalibrated with the various gases used in the study. The Brooks mass flow controller provided a flow accuracy of about ±1.5% of full scale

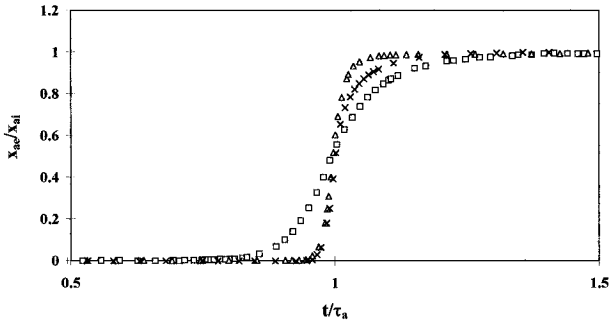


**Figure 2.** Hydrocarbon breakthrough in an activated carbon bed (299.15 K): □, methane, partial pressure 0.13 bar, $v_i = 1.56$ cm/s; △, ethane, partial pressure 0.10 bar, $v_i = 1.28$ cm/s; ×, propane, partial pressure 0.51 bar, $v_i = 1.99$ cm/s.

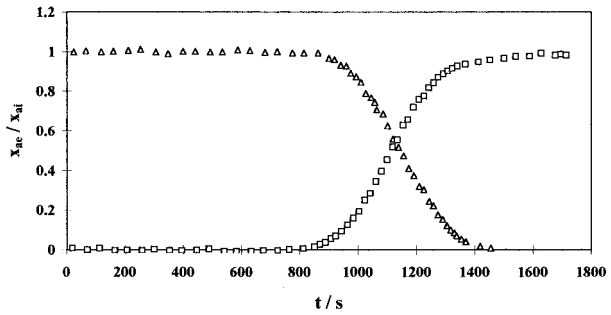


**Figure 3.** Adsorption and desorption breakthrough curves of methane in activated carbon (partial pressure 0.012 bar, 299.15 K): □, adsorption; △, desorption.

**Table 1. Properties of the Adsorbent and Adsorbent Bed**

| | |
|---|---|
| Adsorbent: Activated Carbon (Source: Singapore Refining Co. Ltd.) | |
| apparent density | 0.87 g $cm^{-3}$ |
| particle porosity | 0.58 |
| mean pore radius | $18 \times 10^{-10}$ m |
| specific surface area | 970 $m^2$ $g^{-1}$ |
| particle sizes | (a) column 1: 2.36−2.80 mm (Tyler equiv 8-mesh and 7-mesh) |
| | (b) column 2: 1.18−1.40 mm (Tyler equiv 16-mesh and 14-mesh) |
| bed void fraction | (a) column 1: 0.3994 |
| | (b) column 2: 0.4180 |
| Adsorbent: Silica Gel (Source: Singapore Refining Co. Ltd.) | |
| apparent density | 1.15 g $cm^{-3}$ |
| particle porosity | 0.44 |
| mean pore radius | $20 \times 10^{-10}$ m |
| specific surface area | 666 $m^2$ $g^{-1}$ |
| particle sizes | (a) column 1: 2.36−2.80 mm (Tyler equiv 8-mesh and 7-mesh) |
| bed void fraction | (a) column 1: 0.3612 |

(including the control/readout device accuracy). Flow through the Porter controller was calibrated before each run using a soap bubble meter. This allowed an accuracy of better than ±0.5%. The use of the three mass flow controllers together with four solenoid valves permitted various flow configurations and a wide range of adsorbate concentrations and velocities to be studied.

The other process parameter that needs to be controlled is pressure. One obvious way is to include a separate control loop for the pressure control. In this case, a pressure sensor can be connected to a variable actuating valve at the column outlet. However, a highly accurate control system would then be required since the valve coefficients involved in laboratory-scale experiments are generally very low. As such the control systems would be expensive. As a practical cheaper alternative, a spring-and-diaphragm type back pressure regulator (Go Inc. BP-3) was used for pressure control. Pressure in the system was measured using a calibrated pressure gauge, providing an accuracy of about ±2%.

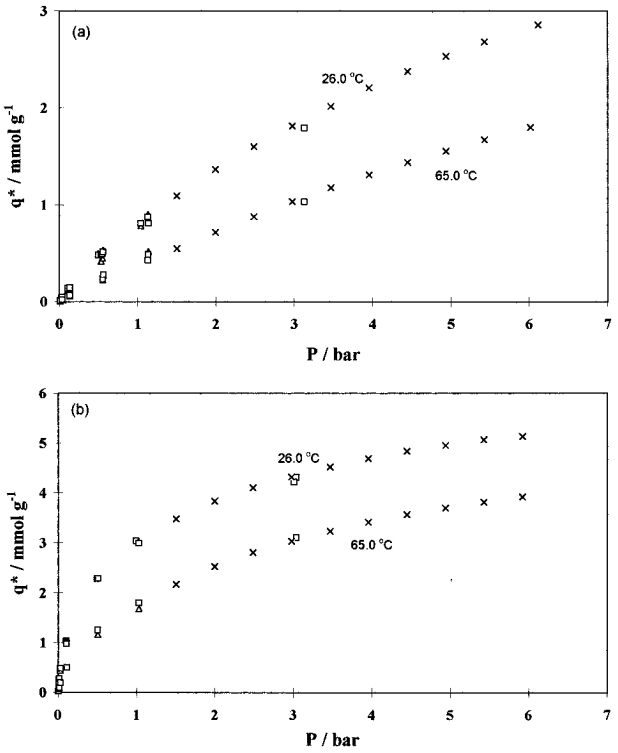


**Figure 4.** Equilibrium isotherms in activated carbon for (a) methane and (b) ethane: □, DCBT adsorption; △, DCBT desorption; ×, CFED.

The exit concentration of adsorbate was measured using a temperature-controlled Shimadzu GC-8A thermal conductivity detector (TCD), which had been precalibrated for the different adsorbates used in the study.

The DCBT and CFED experiments conducted in this study were automated using an Intel 486-based personal computer (PC). The system comprises two variable gain data acquisition and control cards, namely, a software-programmable Keithly Metrabyte V/F conversion card (Chrom-1AT) for accurately reading the voltage output from the TCD and a 12-bit ADDA card to read and control the mass flow controllers. The Chrom-1AT card provided excellent accuracy and noise suppresion, allowing voltage readings of well within ±0.1% of full scale (1 V). The switching of adsorbate and carrier gas flows in the process using solenoid valves was achieved through the use of two double-pole−double-throw relay switches from the Chrom-1AT, while remote set-point control of the flow controllers was achieved using the ADDA card. The use of remote set-point signaling of the mass flow controllers allowed accurate control of the feed velocity during the step changes. As mentioned earlier, it is advantageous to maintain a constant feed velocity during the step changes to minimize hydrodynamic disturbances in the column, particularly for high sorbate concentrations. Due to the need for multiple data acquisition cards and input and output signals as well as real-time flow controls, real-time data acquisition and control software was custom-designed, using event-driven Visual Basic, to run in the Microsoft Windows environment. The whole system allows excellent data acquisition rates, although sampling rates not exceeding 5 Hz were sufficient for the adsorption and desorption experiments conducted here.

In this study, the adsorbates used were pure methane (100%), ethane (100%), and propane (99.5%). The small

**Table 2. Methane, Ethane, and Propane Partial Pressure, *P*, and Amount Adsorbed, *q**, on Activated Carbon**

| *T*/K | *P*/bar | *q**/(mmol g$^{-1}$) | *T*/K | *P*/bar | *q**/(mmol g$^{-1}$) | *T*/K | *P*/bar | *q**/(mmol g$^{-1}$) |
|---|---|---|---|---|---|---|---|---|
| | | | | Methane | | | | |
| 299.15 | 0.0101 | 0.0132 | 318.15 | 0.0116 | 0.0082 | 338.15 | 0.0116 | 0.0062 |
| | 0.0116 | 0.0146 | | 0.0340 | 0.0280 | | 0.0118 | 0.0056 |
| | 0.0305 | 0.0426 | | 0.1334 | 0.0902 | | 0.0354 | 0.0191 |
| | 0.0354 | 0.0464 | | 0.5547 | 0.3288 | | 0.1339 | 0.0617 |
| | 0.0356 | 0.0448 | | 1.1301 | 0.5742 | | 0.5547 | 0.2307 |
| | 0.1049 | 0.1384 | | 1.5038 | 0.7665 | | 0.5624 | 0.2790 |
| | 0.1114 | 0.1356 | | 1.9943 | 0.9701 | | 1.1301 | 0.4261 |
| | 0.1332 | 0.1457 | | 2.4848 | 1.1671 | | 1.1353 | 0.4870 |
| | 0.1345 | 0.1437 | | 2.9753 | 1.3455 | | 1.5038 | 0.5480 |
| | 0.4978 | 0.4804 | | 3.1300 | 1.3472 | | 1.9943 | 0.7169 |
| | 0.5328 | 0.4754 | | 3.4658 | 1.5114 | | 2.4848 | 0.8803 |
| | 0.5508 | 0.4902 | | 3.9563 | 1.6732 | | 2.9753 | 1.0356 |
| | 0.5556 | 0.5137 | | 4.4468 | 1.8262 | | 3.1300 | 1.0325 |
| | 1.0409 | 0.8114 | | 4.9373 | 1.9566 | | 3.4658 | 1.1760 |
| | 1.1311 | 0.8781 | | 5.428 | 2.0855 | | 3.9563 | 1.3102 |
| | 1.1407 | 0.8119 | | 5.91825 | 2.2090 | | 4.4468 | 1.4395 |
| | 1.5038 | 1.0943 | | | | | 4.9373 | 1.5560 |
| | 1.9943 | 1.3648 | | | | | 5.4278 | 1.6720 |
| | 2.4848 | 1.6006 | | | | | 6.0164 | 1.7995 |
| | 2.9753 | 1.8163 | | | | | | |
| | 3.1300 | 1.7942 | | | | | | |
| | 3.4658 | 2.0173 | | | | | | |
| | 3.9563 | 2.2109 | | | | | | |
| | 4.4468 | 2.3794 | | | | | | |
| | 4.9373 | 2.5332 | | | | | | |
| | 5.4278 | 2.6817 | | | | | | |
| | 6.1145 | 2.8560 | | | | | | |
| | | | | Ethane | | | | |
| 299.15 | 0.0082 | 0.2072 | 318.15 | 0.0264 | 0.2807 | 338.15 | 0.0025 | 0.0268 |
| | 0.0131 | 0.2769 | | 0.5119 | 1.7107 | | 0.0079 | 0.0664 |
| | 0.0264 | 0.4358 | | 1.0305 | 2.3048 | | 0.0126 | 0.0946 |
| | 0.0268 | 0.4817 | | 1.5038 | 2.7452 | | 0.0291 | 0.1934 |
| | 0.1003 | 1.0338 | | 1.9943 | 3.0946 | | 0.1080 | 0.4982 |
| | 0.1042 | 1.0006 | | 2.4848 | 3.3761 | | 0.5045 | 1.2504 |
| | 0.1048 | 0.9746 | | 2.9753 | 3.6124 | | 1.0305 | 1.7998 |
| | 0.4972 | 2.2799 | | 3.4658 | 3.8053 | | 1.5038 | 2.1688 |
| | 0.5091 | 2.2872 | | 3.9563 | 3.9823 | | 1.9943 | 2.5320 |
| | 0.9949 | 3.0373 | | 4.4468 | 4.1385 | | 2.4848 | 2.8043 |
| | 1.0305 | 2.9913 | | 4.9373 | 4.2709 | | 2.9753 | 3.0377 |
| | 1.5038 | 3.4786 | | 5.4278 | 4.3910 | | 3.0384 | 3.1079 |
| | 1.9943 | 3.8392 | | 5.9183 | 4.4992 | | 3.4658 | 3.2378 |
| | 2.4848 | 4.1078 | | | | | 3.9563 | 3.4186 |
| | 2.9753 | 4.3248 | | | | | 4.4468 | 3.5700 |
| | 3.0066 | 4.3074 | | | | | 4.9373 | 3.7015 |
| | 3.0384 | 4.2197 | | | | | 5.4278 | 3.8196 |
| | 3.4658 | 4.5211 | | | | | 5.9183 | 3.9220 |
| | 3.9563 | 4.6895 | | | | | | |
| | 4.4468 | 4.8362 | | | | | | |
| | 4.9373 | 4.9558 | | | | | | |
| | 5.4278 | 5.0667 | | | | | | |
| | 5.9183 | 5.1347 | | | | | | |
| | | | | Propane | | | | |
| 299.15 | 0.0172 | 1.0774 | 318.15 | 0.0986 | 1.7546 | 338.15 | 0.0102 | 0.2952 |
| | 0.1009 | 2.2313 | | 1.0214 | 3.4859 | | 0.0269 | 0.6835 |
| | 0.1012 | 2.2835 | | | | | 0.1009 | 1.2946 |
| | 0.5052 | 3.1939 | | | | | 0.1012 | 1.3977 |
| | 1.044 | 3.8675 | | | | | 0.5021 | 2.3628 |
| | | | | | | | 1.0052 | 2.9858 |
| | | | | | | | 1.5086 | 3.3236 |

amount of impurity in the propane used was ethane and thus can be neglected, since it is displaced by propane during adsorption. Table 1 shows the properties of the activated carbon and silica gel used as adsorbents in this study. Helium, which is practically inert to the adsorbent, was used as the carrier gas. The bed of adsorbent was periodically regenerated to maintain its maximum capacity. For activated carbon, the regeneration was performed by leaving the packed column in an oven at 150 °C for 24 h, with helium flowing in the bed, while for silica gel, the temperature was maintained at 120 °C.

The apparatus used for DCBT experiments described above can be easily configured for CFED experiments. In particular, all that is needed is to shut off the inlet flow upon saturation of the bed and to route the exit flow through one of the mass flow controllers to begin the desorption process.

## Experimental Results

***DCBT Method.*** Figure 2 shows typical breakthrough curves of methane, ethane, and propane in activated carbon. The lowest concentration experiment conducted for methane (0.012 bar of partial pressure) in activated carbon showed that it is close to the linear range, as indicated by the near mirror image of the adsorption and desorption breakthrough curves in Figure 3. However,

**Table 3. Methane, Ethane, and Propane Partial Pressure, *P*, and Amount Adsorbed, *q**, on Silica Gel**

| *T*/K | *P*/bar | *q**/(mmol g$^{-1}$) | *T*/K | *P*/bar | *q**/(mmol g$^{-1}$) | *T*/K | *P*/bar | *q**/(mmol g$^{-1}$) |
|---|---|---|---|---|---|---|---|---|
| | | | | Methane | | | | |
| 299.15 | 0.0283 | 0.0042 | 318.15 | 0.4802 | 0.0519 | 338.15 | 0.0290 | 0.0024 |
| | 0.4802 | 0.0798 | | 0.4988 | 0.0518 | | 0.4802 | 0.0405 |
| | 0.4988 | 0.0835 | | 0.9200 | 0.1008 | | 0.8378 | 0.0710 |
| | 0.9387 | 0.1349 | | 1.5038 | 0.1584 | | 1.5038 | 0.1165 |
| | 1.5038 | 0.2011 | | 1.9943 | 0.1990 | | 1.9943 | 0.1524 |
| | 1.9943 | 0.2550 | | 2.9753 | 0.2822 | | 2.9753 | 0.2242 |
| | 2.9753 | 0.3572 | | 3.9563 | 0.3562 | | 3.9563 | 0.2911 |
| | 3.9563 | 0.4531 | | 4.9373 | 0.4213 | | 4.9373 | 0.3442 |
| | 4.9373 | 0.5391 | | 5.9183 | 0.4748 | | 5.9183 | 0.3925 |
| | 5.9183 | 0.6080 | | | | | | |
| | | | | Ethane | | | | |
| 299.15 | 0.0127 | 0.0137 | 318.15 | 0.5052 | 0.2520 | 338.15 | 0.0110 | 0.0058 |
| | 0.5052 | 0.3914 | | 1.0085 | 0.4632 | | 0.5052 | 0.1699 |
| | 0.9965 | 0.6371 | | | | | 1.0204 | 0.3139 |
| | 1.5038 | 0.7985 | | | | | 1.5038 | 0.4136 |
| | 1.9943 | 0.8850 | | | | | 1.9943 | 0.4961 |
| | 2.9753 | 1.0205 | | | | | 2.9753 | 0.6162 |
| | 3.9563 | 1.1205 | | | | | 3.9563 | 0.7071 |
| | 4.9373 | 1.2033 | | | | | 4.9373 | 0.7783 |
| | 5.8202 | 1.2663 | | | | | 5.9183 | 0.8436 |
| | | | | Propane | | | | |
| 299.15 | 0.0074 | 0.0302 | 318.15 | 0.2600 | 0.3749 | 338.15 | 0.0076 | 0.0088 |
| | 0.5098 | 0.8782 | | 1.0118 | 1.0232 | | 0.5098 | 0.4106 |
| | 1.0118 | 1.4340 | | | | | 1.0118 | 0.7133 |

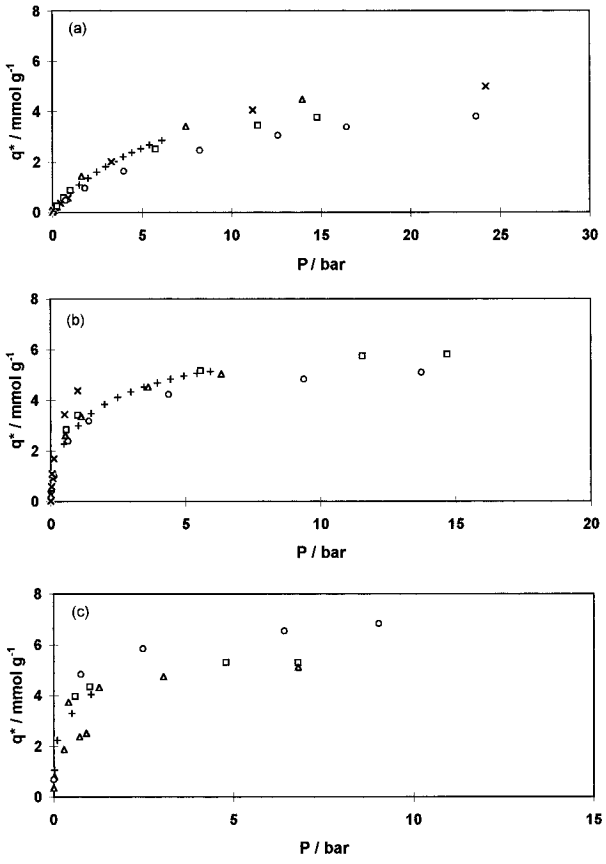


**Figure 5.** Comparison of equilibrium isotherms measured in the present study with published data: (a) methane in activated carbon; □, Ray and Box (*3*); △, Payne *et al.* (*4*); ○, Reich *et al.* (*5*); ×, Yang and Saunders (*6*); +, this work (299.15 K); (b) ethane in activated carbon; □, Ray and Box (*3*); △, Szepesy and Illes (*7*); ○, Reich *et al.* (*5*); ×, Kuro-Oka *et al.* (*8*); +, this work (299.15 K); (c) propane in activated carbon; □, Ray and Box (*3*); △, Szepesy and Illes (*7*); ○, Lewis *et al.* (*9*); ×, Payne *et al.* (*4*); +, this work (299.15 K). Adsorbent details for this work are given in Table 1; adsorbent and experimental details for the other studies are given in Table 4.

both the ethane and propane runs were in the nonlinear range of the isotherm even in the lowest concentration experiments. This was evident from the asymmetry of the adsorption and desorption breakthrough curves.

On the basis of these breakthrough curves, the equilibrium isotherms for these gases in activated carbon and silica gel were derived. Figure 4 shows the experimental isotherm results for methane and ethane at two different temperatures. The isotherm data shown span a moderate hydrocarbon partial pressure range. The isotherm data shown include the equilibrium results obtained using two different bed interstitial velocities and two different adsorbent particle sizes. The use of jacketed columns allowed convenient measurement of the isotherms at different temperatures. Of particular importance is that the equilibrium results for adsorption and desorption were fairly equal, indicating the absence of any hysteresis in the isotherms for the range of pressures studied. It should be mentioned that the equilibrium results at the higher pressures had been corrected using the mean residence time definition given by eq 16. If the conventional definition of mean residence time (eq 1) had been used, the isotherm results for the activated carbon bed would have been lower by as much as 20% (*1*).

***CFED Method.*** The CFED method was used to extend the isotherm results of methane and ethane to higher pressures. This was achieved by extending the results at approximately 1.5 bar obtained using the DCBT method given earlier. The resulting isotherms for methane and ethane are shown in Figure 4. It is apparent that the results from the two methods are in good agreement.

Tables 2 and 3 give the numerical values of the equilibrium data for all three hydrocarbons in activated carbon and silica gel for the three different temperatures used in this study.

***Comparisons with Published Equilibrium Data.*** Activated carbon adsorbents are widely used for hydrocarbon adsorption processes. Indeed, there are a number of published results of light hydrocarbon adsorption in activated carbon. However, these results do not generally provide experimental equilibrium data at the same temperatures. Furthermore, the equilibrium data are highly dependent on the type of activated carbon used. Even so, it would be interesting to compare the results obtained in this study with published data.

**Table 4. Adsorbent and Experimental Conditions for the Equilibrium Results in Figure 5**

| data source | adsorbent | isotherm temp/K |
|---|---|---|
| Ray and Box (*3*) | Columbia Grade L ($1152\ m^2\ g^{-1}$) | 310.92 |
| Payne et al. (*4*) | Columbia Grade G ($1157\ m^2\ g^{-1}$) | 303.15 |
| Reich et al. (*5*) | BPL; Pittsburgh Chemical Co. ($988\ m^2\ g^{-1}$) | 301.4 |
| Yang and Saunders (*6*) | PCB | 295.15 |
| Szepesy and Illes (*7*) | Nuxit-Al ($\cong 1100\ m^2\ g^{-1}$) | 293.15 |
| Kuro-Oka et al. (*8*) | KF-1500 Fiber Carbon ($1440\ m^2\ g^{-1}$) | 298.15 |
| Lewis et al. (*9*) | Black Pearls I ($705\ m^2\ g^{-1}$) | 298.15 |

Figure 5 shows a comparison of the equilibrium results obtained in a number of experiments for the adsorption of methane, ethane, and propane in various types of activated carbon. Table 4 provides the details of the activated carbon used and the experimental temperatures. In the case of methane adsorption, the results of Yang and Saunders (*6*) and Payne et al. (*4*) are very close to those obtained in this work. The data of Ray and Box (*3*) are consistently lower than the others, which may be due to the higher temperature used in their experiment. Interestingly, however, the data of Reich et al. (*5*) are very low even though the experiments were conducted at about the same temperature as this work, and the adsorbent had about the same specific surface area.

For ethane, the data of Szepesy and Illes (*7*) are similar to those from our work, while the data of Reich et al. (*5*) are somewhat lower. As a matter of interest, the data of Kuro-Oka et al. (*8*) for ethane adsorption in the KF-1500 Fiber Carbon are included. This adsorbent has a large specific surface area of 1440 $m^2/g$, which is almost 50% greater than the specific surface area of conventional granular activated carbon adsorbent. This increase in the surface area results in a tremendous difference in the equilibrium capacity of the adsorbent.

Published results of equilibrium data for propane show a greater discrepancy than for the other two hydrocarbons. As in ethane adsorption, the data of Szepesy and Illes (*7*) are comparable to the results found in this study. Of interest are the large equilibrium values reported by Lewis et al. (*9*) for the Black Pearls I adsorbent, although it has a low specific surface area of 705 $m^2/g$.

## Conclusions

The equilibrium results for methane, ethane, and propane in activated carbon and silica gel were obtained using the dynamic column breakthrough method and the constant flow, equilibrium desorption method. The two methods were found to be very effective for measuring single-component adsorption equilibrium data, and they gave consistent results for the systems studied.

## Literature Cited

(1) Malek, A.; Farooq, S.; Rathor, M. N.; Hidajat, K. *Chem. Eng. Sci.* **1995**, *50*, 737−740.
(2) Ruthven, D. M. *Principles of Adsorption and Adsorption Processes*; Wiley: New York, 1984.
(3) Ray, G. C.; Box, E. O. *Ind. Eng. Chem.* **1950**, *42*, 1315.
(4) Payne, H. K.; Sturdevant, G. A.; Leland, T. W. *Ind. Eng. Chem. Fundam.* **1968**, *7*, 363.
(5) Reich, R.; Ziegler, W. T.; Rogers, K. A. *Ind. Eng. Chem. Process Des. Dev.* **1980**, *19*, 336.
(6) Yang, R. T.; Saunders, J. T. *Fuel* **1985**, *64*, 616.
(7) Szepesy, L.; Illes, V. *Acta. Chim. Hung.* **1963**, *35*, 37.
(8) Kuro-Oka, M.; Suzuki, T.; Nitta, T.; Katayama, T. *J. Chem. Eng. Jpn.* **1984**, *17*, 588.
(9) Lewis, W. K.; Gilliland, E. R.; Chertow, B.; Hoffman, W. *J. Am. Chem. Soc.* **1950**, *72*, 1153.

Received for review July 19, 1995. Accepted September 20, 1995.[⊗]

JE950178E

[⊗] Abstract published in *Advance ACS Abstracts*, November 1, 1995.